

# Development and characterisation of a low-concentration sodium dodecyl sulphate decellularised porcine dermis

Journal of Tissue Engineering  
Volume 8: 1–12  
© The Author(s) 2017  
Reprints and permissions:  
sagepub.co.uk/journalsPermissions.nav  
DOI: 10.1177/2041731417724011  
journals.sagepub.com/home/tej



Jack A Helliwell<sup>1</sup>, Daniel S Thomas<sup>1</sup>, Vaia Papathanasiou<sup>2</sup>,  
Shervanthi Homer-Vanniasinkam<sup>2</sup>, Amisha Desai<sup>1</sup>,  
Louise M Jennings<sup>1</sup>, Paul Rooney<sup>3</sup>, John N Kearney<sup>3</sup>  
and Eileen Ingham<sup>1</sup>

## Abstract

The aim of this study was to adapt a proprietary decellularisation process for human dermis for use with porcine skin. Porcine skin was subject to: sodium chloride (1 M) to detach the epidermis, trypsin paste to remove hair follicles, peracetic acid (0.1% v/v) disinfection, washed in hypotonic buffer and 0.1% (w/v) sodium dodecyl sulphate in the presence of proteinase inhibitors followed by nuclease treatment. Cellular porcine skin, decellularised porcine and human dermis were compared using histology, immunohistochemistry, GSL-1 lectin (alpha-gal epitope) staining, biochemical assays, uniaxial tensile and in vitro cytotoxicity tests. There was no microscopic evidence of cells in decellularised porcine dermis. DNA content was reduced by 98.2% compared to cellular porcine skin. There were no significant differences in the biomechanical parameters studied or evidence of cytotoxicity. The decellularised porcine dermis retained residual alpha-gal epitope. Basement membrane collagen IV immunostaining was lost following decellularisation; however, laminin staining was retained.

## Keywords

Dermis, decellularisation, skin, xenograft

Date received: 25 April 2017; accepted: 12 July 2017

## Introduction

The estimated prevalence of chronic non-healing leg ulcers in the United Kingdom is between 1.5 and 3 per 1000 population.<sup>1</sup> For a number of patients, conventional treatment options have proven largely ineffective.<sup>2</sup> This has led to alternative treatment options being sought, including the use of acellular dermal matrices.

Acellular dermal scaffolds have been reported to improve the wound-healing environment and regulate cell behaviour by replacing the damaged extracellular matrix (ECM) and providing a scaffold to support cell in-growth.<sup>3</sup> The high levels of matrix metalloproteinases (MMPs) present in the chronic wound environment are believed to break down collagen in the dermal scaffold, releasing bound growth factors. This has been suggested to lead to a rebalance of proteases and growth factors, which in turn results in reduced inflammation and increased cell in-growth and angiogenesis.<sup>3</sup>

An acellular allogeneic dermal matrix has been produced from human split-thickness cadaveric donor skin, using a proprietary method of decellularisation.<sup>4</sup> This method incorporates the use of low-concentration sodium dodecyl sulphate (SDS) and proteinase inhibitors and has been used to decellularise a range of tissues including porcine bladder, meniscus and cartilage.<sup>5–7</sup> The process has been shown to remove the cellular components, while

<sup>1</sup>Institute of Medical and Biological Engineering, University of Leeds, Leeds, UK

<sup>2</sup>Leeds Vascular Institute, Leeds General Infirmary, Leeds, UK

<sup>3</sup>Tissue and Eye Services, NHS Blood and Transplant, Liverpool, UK

### Corresponding author:

Eileen Ingham, Institute of Medical and Biological Engineering, University of Leeds, LS2 9JT Leeds, UK.  
Email: e.ingham@leeds.ac.uk



effectively preserving the integrity of the ECM. This decellularised human dermis has been used to successfully treat cutaneous wounds following just a single application. In a pilot study, 20 patients with treatment-resistant ulcers underwent hydrosurgical debridement, application of decellularised human dermis and negative pressure dressing for 1 week. The wound surface area decreased in all patients after treatment with a mean reduction of 87% after 6 months and 60% healed completely.<sup>8</sup> A second study compared the angiogenic response in acute cutaneous human wounds treated with decellularised human dermis, collagen-glycosaminoglycans (GAGs) scaffold or autograft. The study found that treatment with decellularised human dermis resulted in increased angiogenesis.<sup>9</sup>

In light of these positive clinical results, it was hypothesised that the decellularisation process could be used to produce an acellular porcine dermis, without adversely affecting the biological, biochemical or biomechanical properties of the tissue. The aim of this study was therefore to develop a method for the decellularisation of porcine dermis, based on the use of low-concentration SDS and proteinase inhibitors. Once a decellularisation protocol was developed for porcine dermis, the acellular dermal matrix was characterised and compared to native cellular porcine skin and decellularised human dermis.

## Materials and methods

### Tissue procurement

Full-thickness porcine skin, dissected from the backs of Large White pigs (circa 6 months old), was supplied within 4 h of slaughter from a local abattoir (M&C Meats, Marshal Street abattoir, Leeds, UK). Skin from a total of six pigs was used in this study.

Decellularised human dermis from each of three donors was supplied by NHS Blood and Transplant Tissue and Eye Services.<sup>10</sup>

### Reagents

The following reagents were used during decellularisation: sodium chloride (Thermo Fisher Scientific), Dulbecco's phosphate-buffered saline (PBS) tablets (Oxoid), low melting point agarose (Invitrogen), trypsin (Sigma), trypsin inhibitor (Sigma), disodium ethylenediaminetetraacetic acid (EDTA; Thermo Fisher Scientific), aprotinin (100000 KIU/mL; Mayfair house), peracetic acid (PAA; Sigma Aldrich), trizma base (Sigma Aldrich), SDS (Sigma Aldrich), benzonase nuclease HC (Merck, Novagen), magnesium chloride (Thermo Fisher Scientific), hydrochloric acid (6M; VWR International) and sodium hydroxide (6M; Thermo Fisher Scientific). All other chemicals were obtained from Sigma Aldridge, Poole, UK, unless otherwise stated.

### Decellularisation protocol for porcine dermis

The protocol developed for the decellularisation of porcine dermis is shown in Table 1. This protocol was used to produce 30 replicate samples of decellularised porcine dermis (6 cm × 4 cm) from each of three different porcine donors.

A total of 30 replicate control samples (6 cm × 4 cm) of split thickness (700 µm) cellular porcine skin were obtained from each of the same three porcine donors following treatment using steps (1) and (2) in Table 1. The control samples were cryopreserved at -80°C until required using a controlled freezing rate. Samples were placed in a nylon bag with cryopreservation medium (Hanks' balanced salt solution containing 0.011 g/L phenol red supplemented with 25 mM HEPES and 15% v/v dimethyl sulphoxide), wrapped in foil, placed in a jiffy bag and then cardboard box.

### Histological evaluation

Three replicate samples of cellular split-thickness porcine skin, decellularised porcine dermis from each pig and decellularised human dermis from each human donor were processed for wax histology and sectioned (5 µm) using standard methods. Sections were dewaxed in xylene and rehydrated through a graded series of alcohols to water. The sections were then stained with haematoxylin and eosin (H&E) to assess the general structure of the tissue. Sections were also stained using Miller's stain for visualisation of elastin and then counterstained with Sirius red or Van Gieson to visualise the collagen fibres.<sup>6</sup>

### Immunohistochemical analysis of basement membrane proteins

Collagen IV and laminin were labelled using specific monoclonal antibodies: mouse anti-collagen IV (manufacturer: DAKO MO785, clone: CIV22, isotype: mouse IgG1) and mouse anti-laminin (manufacturer: Sigma L8271, clone: LAM-89, isotype: mouse IgG1) to determine the presence of basement membrane proteins. The same antibody was used for both porcine and human tissues. Three replicate samples of cellular porcine split-thickness skin, decellularised porcine dermis and decellularised human dermis from three pigs and three human donors were analysed. Paraffin wax sections (5 µm) were dewaxed with xylene and rehydrated using a graded series of alcohols to water. When labelling collagen IV, heat-mediated antigen retrieval was performed by covering sections with 10 mM citric acid (VWR International; pH 6) before heating with a microwave at 800 W for 10 min. When labelling laminin, enzymatic antigen retrieval was carried out by adding one drop of proteinase K (DAKO) to each section for 7 min. Sections were rinsed using PBS before dual endogenous enzyme blocker (Thermo Scientific; Ultra V Block from Ultravision kit) was applied. Primary antibodies were diluted (mouse anti-collagen IV = 1:50; mouse

**Table 1.** Porcine dermis decellularisation protocol.

Step	Process	Time
1	Well Xpert hair clippers were used to remove all visible hairs from the surface of the skin	–
2	Split thickness sections (800–1500 µm) were obtained using an Integra Model B dermatome	–
3	Samples were treated with sodium chloride (1M) at 240 r/min, 37°C. The epidermis was peeled away from the dermis using forceps	18 h
4	Washed in PBS at 240 r/min, 37°C	3 × 20 min
5	Trypsin treatment paste (1.125 × 10 <sup>4</sup> U/mL, 0.5% (w/v) agarose) was applied to the epidermal surface of the dermis and incubated at 37°C to remove hair follicles	2 h
6	Washed in trypsin inhibitor (5000 U/mL trypsin inhibitor, 0.1% (w/v) EDTA and 10 KIU/mL aprotinin)	3 × 30 min
7	Tissue was disinfected in peracetic acid solution (0.1% v/v) at 240 r/min, 25°C	3 h
8	Washed in buffer 1 (PBS, 0.1% (w/v) EDTA, 10 KIU/mL aprotinin) at 240 r/min, 25°C	3 × 20 min
9	Incubated in hypotonic buffer (10 mM Tris, 2.7 mM EDTA, 10 KIU/mL aprotinin) at 240 r/min, 4°C to lyse cells	16 h
10	Washed in detergent buffer (0.1% w/v SDS, 10 mM Tris, 10 KIU/mL aprotinin) at 240 r/min, 25°C to remove cellular fragments	24 h
11	Washed in buffer 2 (PBS, 10 KIU/mL aprotinin)	3 × 30 min
12	Incubated in nuclease buffer (50 mM Tris, 1 mM MgCl <sub>2</sub> ·6H <sub>2</sub> O, 10 KIU/mL Benzonase) at 80 r/min, 37°C	3 h
13	Washed in buffer 1 (PBS, 0.1% (w/v) EDTA, 10 KIU/mL aprotinin) at 240 r/min, 25°C	3 × 20 min

PBS: phosphate-buffered saline.

anti-laminin=1:800) using antibody diluent (Tris-buffered saline (TBS), 0.1% w/v bovine serum albumin (BSA), 0.1% w/v sodium azide), added to the section and incubated for 90 min at room temperature. To control sections, the isotype control was added at the same protein concentration as the primary antibody. To negative control sections, only antibody diluent (TBS, 0.1% w/v BSA, 0.1% w/v sodium azide) was added. The staining was then performed using Ultravision kit (Thermo Scientific).

### Analysis of residual alpha-gal epitope

The alpha-gal epitope was labelled using biotinylated GSL-1 – isolectin B<sub>4</sub> (GSL-1 Lectin; Vector laboratories). Three samples of cellular split-thickness porcine skin, decellularised porcine dermis and decellularised human dermis from three pigs and three human donors were analysed. Paraffin wax sections (5 µm) were dewaxed in xylene and rehydrated through a graded series of alcohols to water. Antigen unmasking was performed by immersing sections in preheated antigen unmasking solution (Vector laboratories) at 95°C for 25 min. Each section was then covered with streptavidin blocking solution and biotin blocking solution (Vector laboratories), each for 15 min. Non-specific binding was then blocked using CarboFree blocking solution (Vector laboratories) for 30 min. GSL-1 Lectin was diluted to 5 µg/mL, added to each section and incubated for 30 min at room temperature. To control sections, galactose-blocked lectin at the same GSL-1 Lectin concentration (5 µg/mL) was added. This was prepared by diluting GSL-1 Lectin in galactose blocking solution (200 mM, 0.1% sodium azide). GSL-1 Lectin was then

visualised using streptavidin horseradish peroxidase and ImmPACT DAB detection method.

### Determination of DNA content

DNA content was investigated both qualitatively and quantitatively. Histological sections from three replicate samples of cellular split-thickness porcine skin, decellularised porcine dermis and decellularised human dermis from each porcine and human donor were stained using 4',6-diamidino-2-phenylindole dihydrochloride (DAPI) for visualisation of nuclear material.<sup>11</sup> A commercially available kit (DNAeasy kit, Qiagen) was used to isolate the DNA from control split-thickness porcine skin, decellularised porcine dermis and decellularised human dermis. Six replicate samples per pig/donor in each group were processed. Samples were macerated, lyophilised, weighed and processed as per manufacturers' instructions. The levels of extracted DNA were measured by Nanodrop spectrophotometry at 260 nm and expressed as ng/mg dry weight of tissue.

### Determination of hydroxyproline (collagen) content

The hydroxyproline content of six replicate samples per pig/donor in each group was quantified. Lyophilised tissue (15 mg) was acid hydrolysed by adding 5 mL 6M hydrochloric acid to each sample and incubating in a block heater at 80°C for 18 h. Samples were then neutralised (6M NaOH) before 50 µL of each was added to a 96-well plate. Chloramine T (100 µL) was added and the plate shaken gently for 5 min. Ehrlich's reagent (100 µL) was

then added and the plate incubated in an oven at 60°C for 45 min. The optical density of each well was then measured using a micro plate spectrophotometer at 570 nm. The absorbance units were converted to hydroxyproline concentration using a standard curve (produced using known concentrations of hydroxyproline).

### **Biomechanical testing**

Biomechanical properties were investigated by uniaxial tensile testing. Six replicate samples per pig/donor in each group were tested. A custom-made tissue cutter was used to cut rectangular strips (5 mm × 20 mm) from each sample. Thickness was measured using a J-40-V (James H Heal and Company Limited) gauge at six different points along the length and averaged. The tissue was then clamped into a titanium holder, using grips appropriate for soft tissue, with the gauge length set to 10 mm. Once the tissue was secured in the titanium holder, it was placed into an Instron materials testing machine model 3365 and pulled to failure at 10 mm/min. The displacement, force (500 N load cell) and time response were recorded throughout the experiment. The data were transferred to Excel spreadsheet and stress-strain response calculated, along with the following parameters: elastin phase modulus, collagen phase modulus and ultimate tensile strength (UTS). The mean, standard deviation and 95% confidence limits for each parameter was calculated. One-way analysis of variance (ANOVA) was employed for evaluating the existence of difference among the cellular porcine skin, decellularised porcine dermis and decellularised human dermis. A p-value of <0.05 was considered to be statistically significant.

### **In vitro cytotoxicity testing**

Contact cytotoxicity testing was carried out as described previously.<sup>4</sup> A standard contact cytotoxicity assay was used. Four replicate decellularised porcine dermis samples (5 mm<sup>2</sup>) from each porcine donor were tested against two cell types: baby hamster kidney (BHK; Health Protection Agency) cells and L929 (Health Protection Agency) cells, which were seeded into 6-well tissue culture plates and incubated for 48 h in 5% (v/v) CO<sub>2</sub> in air at 37°C. Living cultures, as well as cells fixed with neutral buffered formalin (NBF) and stained with Giemsa, were examined microscopically, observing whether there was growth of cells up to the tissue samples.

## **Results**

### ***Histological evaluation of cellular porcine skin, decellularised porcine dermis and decellularised human dermis***

In histological sections of decellularised porcine dermis stained with H&E, there was no light microscopic evidence

of cells (Figure 1). There was no obvious difference in the structure of the ECM, including distribution of collagen and elastin fibres, between cellular porcine skin and decellularised porcine dermis. The distribution of collagen fibres was particularly evident in Sirius red/Miller's elastin-stained tissue sections, where there was a similar pattern of red-stained collagen fibres (Figure 1). There was also a similar distribution of blue, Miller's elastin-stained elastin fibres, which were more visible in tissue sections stained with Van Gieson/Miller's elastin (Figure 1).

In sections of decellularised human dermis, the distribution of collagen fibres appeared less dense than in the porcine dermis sections (Figure 1). Qualitative assessment of blue, Miller's elastin-stained elastin fibres suggested higher intensity of staining in decellularised human dermis compared to decellularised porcine dermis (Figure 1).

### ***Immunohistochemical analysis of the basement membrane in cellular porcine skin, decellularised porcine dermis and decellularised human dermis***

Staining of cellular porcine skin with anti-collagen IV antibody showed positive staining of the basement membrane and around blood vessels (Figure 2). Following decellularisation, collagen IV staining was no longer visible in decellularised porcine dermis (Figure 2). In decellularised human dermis from one donor, positive collagen IV staining was seen at the basement membrane and around blood vessels (Figure 2). There was no staining for collagen IV evident in the basement membrane and only weak staining around blood vessels in the sections of decellularised dermis from the other two human donors (images not shown).

Sections of cellular porcine skin labelled with anti-laminin antibody showed positive staining of the basement membrane, with limited staining around blood vessels (Figure 2). A similar distribution of staining was seen in decellularised porcine dermis, where laminin remained present at the basement membrane (Figure 2). In decellularised human dermis, positive staining of laminin was visible at the basement membrane and around blood vessels (Figure 2).

### ***Determination of the presence of the alpha-gal epitope***

Labelling the alpha-gal epitope with biotinylated GSL-1 isolectin B<sub>4</sub> in the tissue sections revealed positive staining throughout the dermis and deeper keratinocytes of cellular porcine skin (Figure 2). In decellularised porcine dermis, residual alpha-gal remained present throughout the dermis (Figure 2). Generally, no staining was seen in decellularised human dermis, although small areas of focal staining were visible in tissue sections of dermis from one human donor (Figure 2).



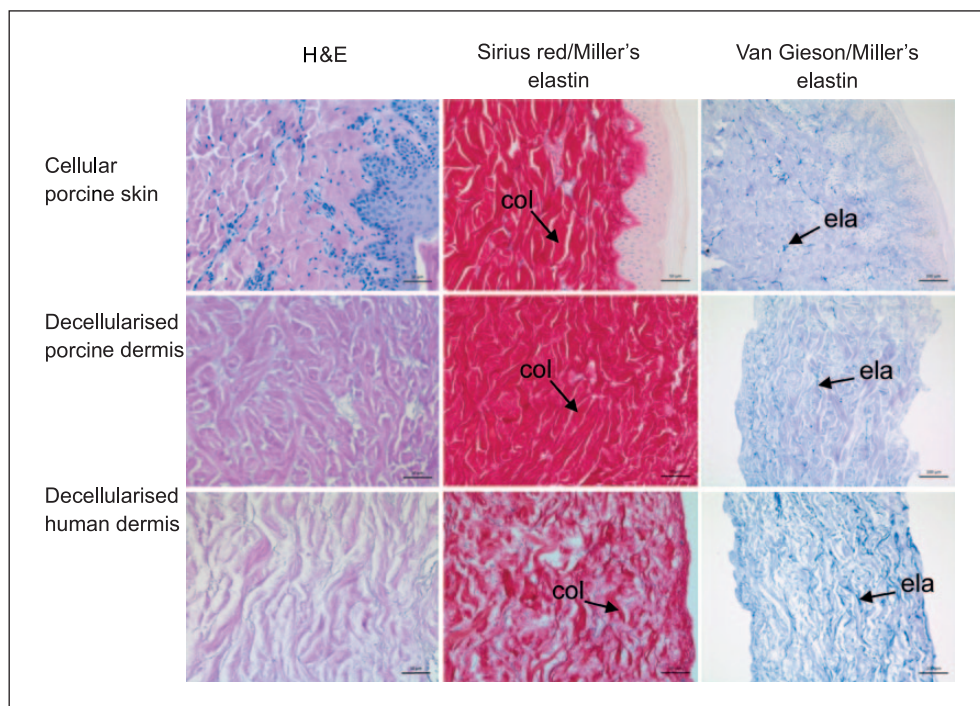


**Figure 1.** Images of histological sections of cellular porcine skin, decellularised porcine dermis and decellularised human dermis. Stained with haematoxylin and eosin showing an absence of visible cell nuclei in decellularised porcine dermis and decellularised human dermis; stained with Sirius red Miller's elastin showing the distribution of collagen fibres (col); stained with Van Gieson Miller's elastin showing the distribution of elastin fibres (ela). Images of H&E and Sirius red Miller's elastin-stained sections captured at 30 $\times$  magnification, with scale bars 50  $\mu$ m. Images of Van Gieson Millers elastin stained sections captured at 20 $\times$  magnification, with scale bars 100  $\mu$ m.

### *Determination of DNA content in cellular porcine skin, decellularised porcine dermis and decellularised human dermis*

DAPI staining of tissue sections indicated the presence of cell nuclei in cellular porcine skin (Figure 3). There was no staining of DNA in the sections of decellularised porcine dermis (Figure 3) or decellularised human dermis (image not shown), in which only background autofluorescence was visible.

The concentration of DNA in cellular porcine skin, decellularised porcine dermis and decellularised human dermis is shown in Table 2. There was a significant reduction in the DNA content of the decellularised porcine dermis compared to cellular porcine skin (one-way ANOVA,  $p < 0.05$ ). The mean percentage DNA remaining in decellularised porcine dermis compared to cellular porcine dermis was 1.8% equivalent to 98.2% DNA removal. There was no significant difference in mean DNA content between decellularised porcine dermis and decellularised human dermis (one-way ANOVA,  $p > 0.05$ ).

### *In vitro cytotoxicity*

When cells were cultured in the presence of samples of decellularised porcine dermis, no zones of inhibition were observed and BHK and L929 cells both grew up to the decellularised porcine dermis (Figure 3). When cells were

cultured in the presence of the positive control of cyanoacrylate glue, cell death and a zone of inhibition was observed (image not shown).

### *Determination of hydroxyproline content in cellular porcine skin, decellularised porcine dermis and decellularised human dermis*

Hydroxyproline concentration is an indicator of collagen content. The concentration of hydroxyproline in cellular porcine skin, decellularised porcine dermis and decellularised human dermis is shown in Figure 4. The mean hydroxyproline concentration in decellularised porcine dermis was significantly higher than cellular porcine skin (one-way ANOVA,  $p < 0.05$ ). There was no significant difference between the hydroxyproline content of decellularised porcine dermis and decellularised human dermis (one-way ANOVA,  $p > 0.05$ ).

### *Biomechanical testing of cellular porcine skin, decellularised porcine dermis and decellularised human dermis*

The calculated biomechanical parameters for cellular porcine skin, decellularised porcine dermis and decellularised human dermis are illustrated in Figure 5.

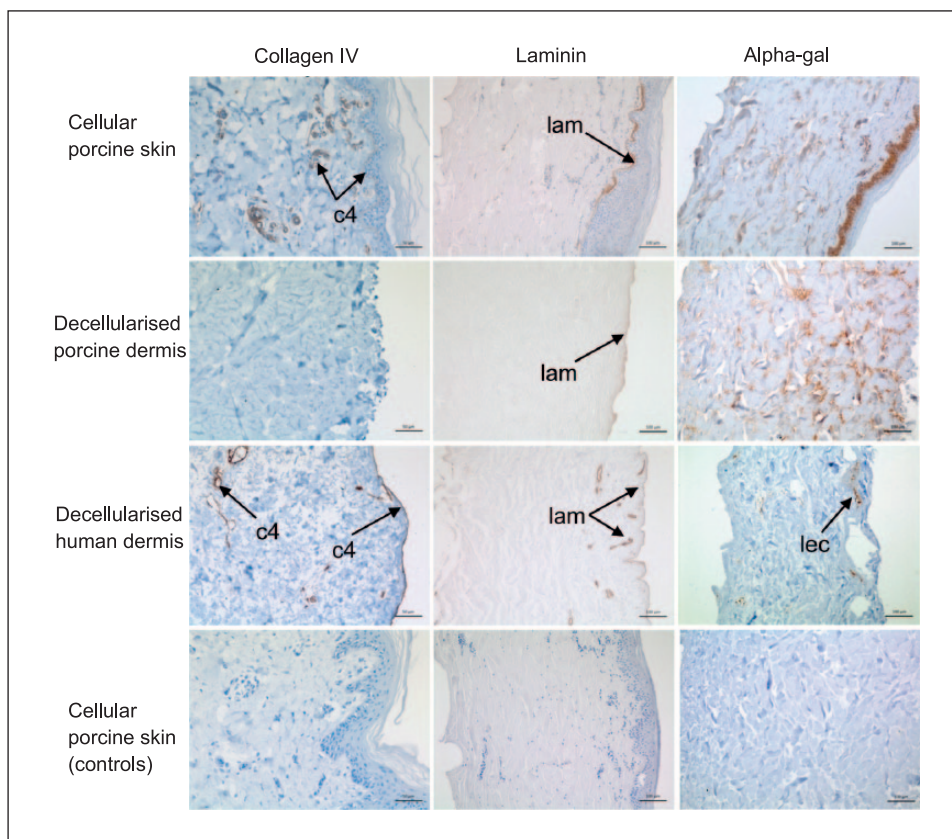


**Figure 2.** Images of histological sections of cellular porcine skin, decellularised porcine dermis and decellularised human dermis stained with anti-collagen IV, anti-laminin and GSL-I isolectin B<sub>4</sub>. The images show positive collagen IV staining (c4) in cellular porcine skin and decellularised human dermis but not in decellularised porcine dermis. Positive laminin staining (lam) was visible in cellular porcine skin, decellularised porcine dermis and decellularised human dermis. Residual alpha-gal remained present throughout the dermis in decellularised porcine dermis. Small areas of focal staining (lec) were visible in decellularised human dermis. The controls (bottom panel) are labelled with isotype control antibodies (collagen IV and laminin) and galactose blocked GSL-I isolectin B<sub>4</sub>. Images of anti-collagen IV stained sections captured at 30× magnification, with scale bar 50 μm. All other images captured at 20× magnification, with scale bar 100 μm.

The results showed no significant differences between cellular porcine skin, decellularised porcine dermis and decellularised human dermis in the biomechanical parameters UTS, collagen phase modulus, elastin phase modulus and maximum load (one-way ANOVA,  $p > 0.05$ ). However, the average thickness of decellularised human dermis was significantly lower than decellularised porcine dermis (one-way ANOVA,  $p < 0.05$ ).

Perusal of the individual data points for each pig/donor revealed there was considerable variation between pigs within the decellularised porcine dermis group (Figure 6). This explained the large error bars when these data were grouped.

## Discussion

### *Development of a protocol for the decellularisation of porcine dermis*

This study aimed to produce a decellularised porcine dermis, using, for the first time, a method of decellularisation

that uses low-concentration 0.1% (w/v) SDS and proteinase inhibitors.

Several methods of decellularisation have been reported in the literature.<sup>12,13</sup> Each process that has been described aims to remove the cells while maintaining the native complex, three-dimensional structure of the ECM. It is, however, recognised that the majority of processes lead to at least some disruption.<sup>12</sup> The proprietary method used in this study incorporates low-concentration 0.1% (w/v) SDS and proteinase inhibitors, which has been shown to effectively remove cells and cellular components, while minimising damage to the ECM.<sup>14,15</sup> This method has been used to decellularise a range of functional animal and human tissues, including human cadaveric donor skin.<sup>4</sup>

The application of the process used to decellularise human skin was found to be inadequate for the decellularisation of porcine skin. The main problem that arose was finding a suitable method for removing the hair and associated hair follicles from the porcine skin. Several approaches for removing the hairs from porcine skin were

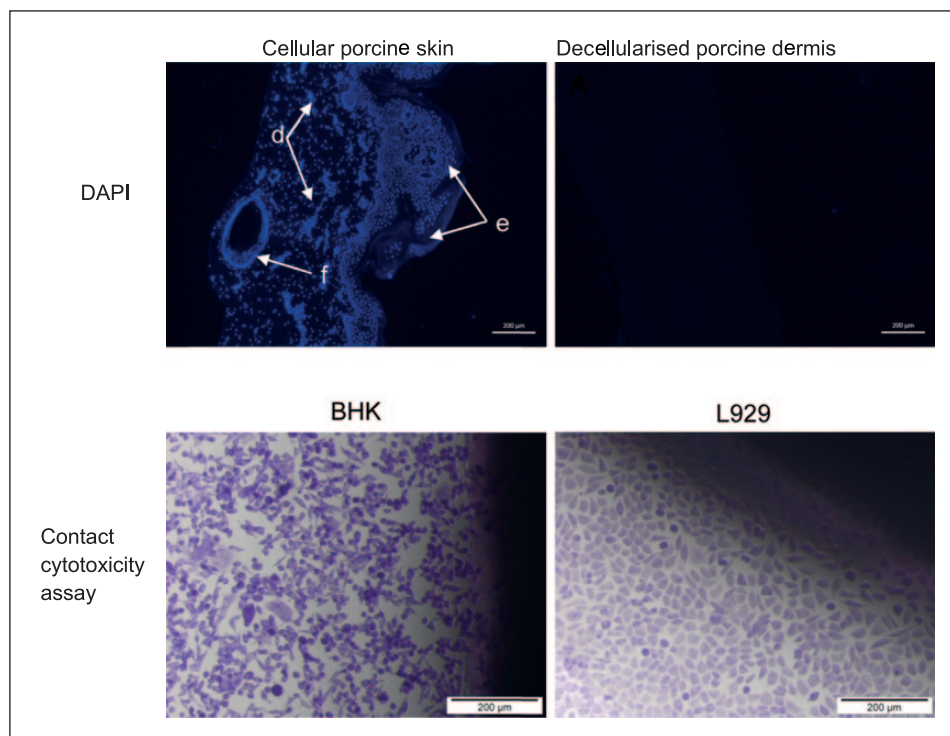


**Figure 3.** Top panel: images of DAPI-stained sections to show the presence of cell nuclei in cellular porcine skin and decellularised porcine dermis. The image of cellular porcine skin shows cell nuclei visible within the dermis (d), epidermis (e) and hair follicle (f). There were no visible cell nuclei in decellularised porcine dermis. Images captured at 10× magnification. Scale bars 200 µm. Bottom panel: images of the cellular appearance of BHK and L929 in the contact cytotoxicity assay. BHK cells and L929 cells exposed to decellularised porcine dermis demonstrate no zones of inhibition. Images captured at 10× magnification. Scale bars 200 µm.

**Table 2.** Comparison of DNA content in cellular porcine skin, decellularised porcine dermis and decellularised human dermis.

		DNA content per pig/donor (ng/mg) Mean, n = 6	DNA content per group (ng/mg) Mean ± 95% CL, n = 3
Cellular porcine skin	Pig 1	1802.79	1809 ± 1153
	Pig 2	793.18	
	Pig 3	2831.29	
Decellularised porcine dermis	Pig 1	23.00	33 ± 17
	Pig 2	49.94	
	Pig 3	24.63	
Decellularised human dermis	Donor 1	65.29	51 ± 14
	Donor 2	46.61	
	Donor 3	42.49	

CL: confidence limits; ANOVA: analysis of variance.

The three groups (cellular porcine skin, decellularised porcine, decellularised human) were compared by one-way ANOVA and post hoc testing (Tukey's procedure). DNA content in decellularised porcine dermis was significantly lower than cellular porcine skin ( $p < 0.05$ ). There was no significant difference between decellularised porcine dermis and decellularised human dermis ( $p > 0.05$ ).

attempted until it was shown that treatment with trypsin paste was effective, enabling the production of an acellular porcine dermis. The use of trypsin treatment paste during other decellularisation processes has been reported, including for the decellularisation of porcine heart valves.<sup>14,15</sup> The trypsin was applied to the epidermal surface as a paste in order to prevent damage to the ECM; however, it is possible that some disruption to the

basement membrane proteins occurred and contributed to the decellularisation process. This final porcine dermis decellularisation protocol involved the following steps: chemical removal of the epidermis using 1 M NaCl, application of trypsin treatment paste to remove hair follicles, PAA disinfection to prevent microbial growth during subsequent washes, lysing of the cells using hypotonic buffer, removal of cellular fragments using detergent buffer and

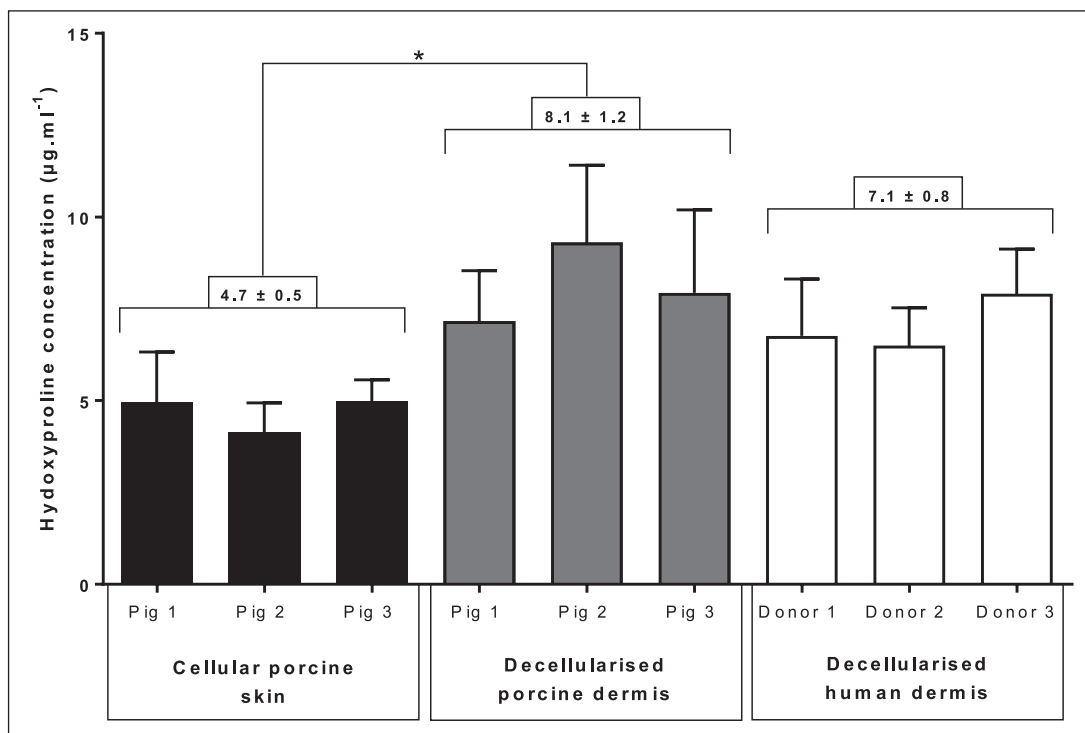


**Figure 4.** Comparison of hydroxyproline content in cellular porcine skin, decellularised porcine dermis and decellularised human dermis.

Each bar represents hydroxyproline concentration per pig/human donor (mean (n=6) ± 95% CL). The figures above the bars indicate the mean hydroxyproline concentration per group (mean (n=3) ± 95% CL) stated above group connectors.

The three groups (cellular porcine, decellularised porcine and decellularised human) were compared by one-way ANOVA and post hoc testing (Tukey's procedure). The asterisk indicates a significant difference between the cellular porcine skin and dCELL porcine dermis (p<0.05).

removal of nucleic acids using nuclease. Histological analysis showed this was a successful process for removal of cells, including those associated with hair follicles. The overall structure of the ECM was maintained and did not appear disrupted by trypsin treatment.

The inclusion of trypsin treatment to remove hair follicles increased the duration of the decellularisation process from approximately 3.5 to 4.5 days.<sup>4</sup> This was acceptable since the process was relatively short compared to some decellularisation processes, such as one method reported for the decellularisation of human trachea, which involved 2–3 cycles of decellularisation over a 10-day period.<sup>16</sup>

#### *Characterisation of the decellularised porcine dermis: comparison with cellular porcine skin and decellularised human dermis*

Once a process for the production of decellularised porcine dermis was established, the study aimed to characterise the acellular porcine dermis produced, in order to determine whether the decellularisation process affected the biological, biochemical or biomechanical properties of the native tissue. In addition to comparing the decellularised porcine dermis to native cellular porcine skin, comparison was also made with the decellularised human

dermis, manufactured by NHS Blood and Transplant Tissue and Eye Services.

The primary objective of any decellularisation process is to remove the cells, in order to prevent an immunological response to cellular antigens upon subsequent implantation. The identification of cellular components, such as DNA, can be used to determine whether cells are still present in biological scaffolds. Histological sections stained with DAPI, a fluorescent stain that binds to AT regions of DNA, indicated there was no staining of DNA in decellularised porcine dermis and decellularised human dermis.

Complete removal of all cellular remnants is unlikely with any method of decellularisation.<sup>17</sup> Quantification of residual DNA can be used as a surrogate marker for determining the effectiveness of a decellularisation process. The DNA content in decellularised porcine dermis was significantly reduced to below 50 ng/mg. Determination of DNA content in decellularised human dermis showed there was no significant difference between the acellular scaffolds. The presence of residual low levels of DNA is not thought to lead to an adverse immunological response.<sup>12</sup>

When considering the possible immunological response to decellularised xenogeneic tissue, it is also important to consider the role of the alpha-gal epitope. Labelling of the alpha-gal epitope with biotinylated GSL-1 isolectin B<sub>4</sub>



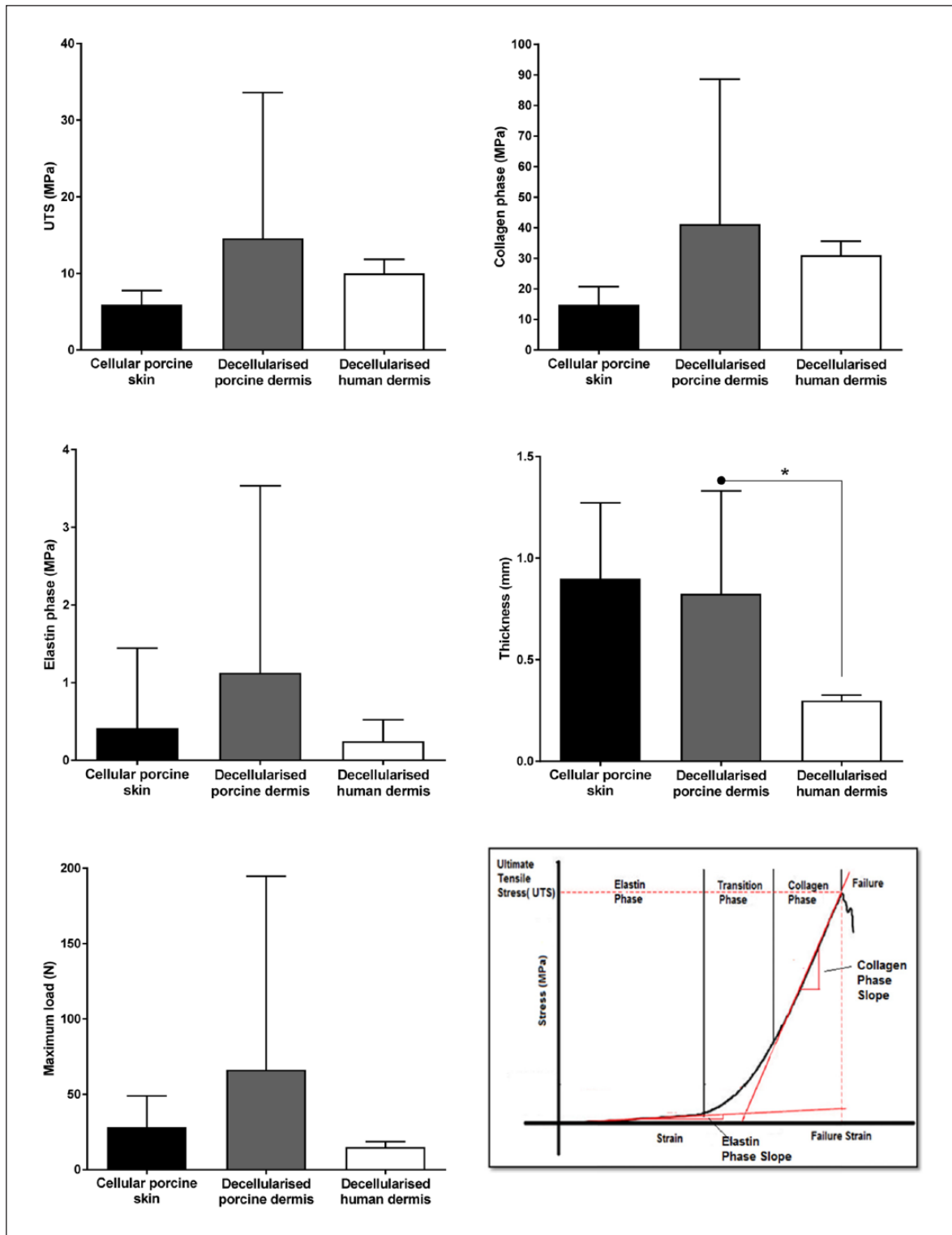


**Figure 5.** Calculated biomechanical parameters for cellular porcine skin, decellularised porcine dermis and decellularised human dermis.

Each bar represents biomechanical parameter per group (mean (n=3) + 95% CL).

Asterisks and connectors indicate significant difference between originator and end arrow column, determined by one-way ANOVA and post hoc testing (Tukey's procedure).

The graph in the bottom right panel shows the typical stress-strain behaviour of the dermis, with tri-phasic characteristics of an elastin phase, transition phase and collagen phase. The elastin phase modulus was taken as the slope of the elastin phase, the collagen phase modulus the slope of the collagen phase, and the ultimate tensile strength was the stress at failure.

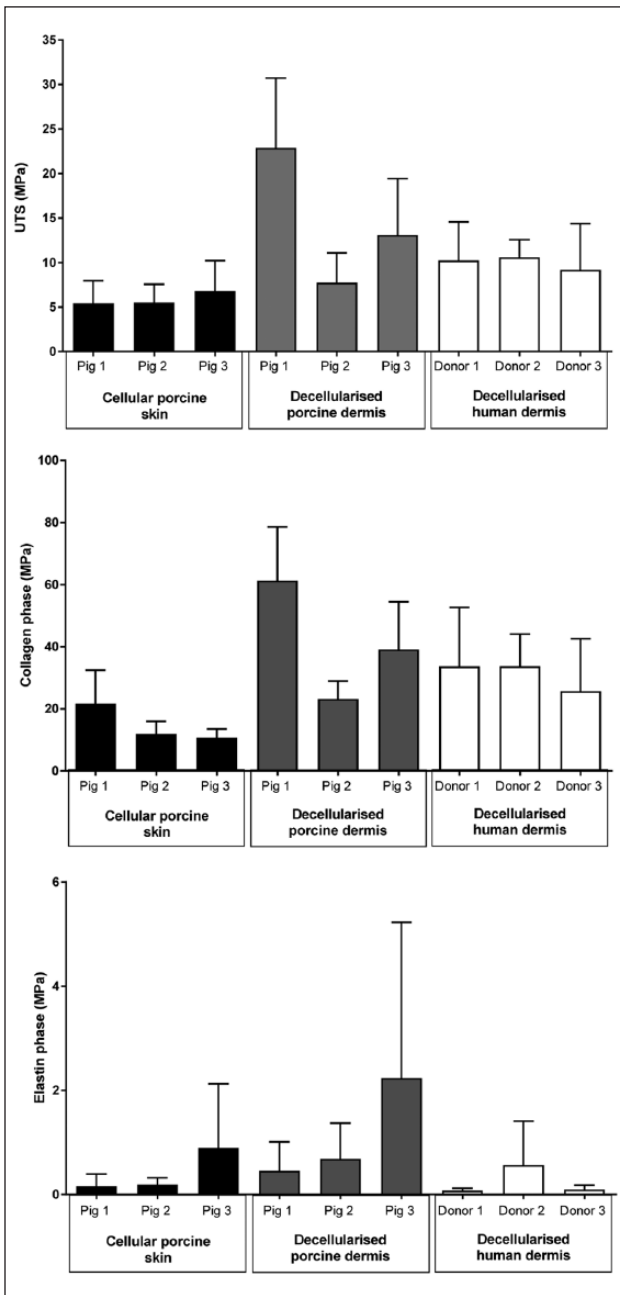


**Figure 6.** Calculated biomechanical parameters for cellular porcine skin, decellularised porcine dermis and decellularised human dermis per pig and human donor. Each bar represents biomechanical parameter per pig/human donor (mean ( $n=6$ ) + 95% CL).

revealed positive staining of residual alpha-gal throughout decellularised porcine dermis. It was not possible to determine whether the alpha-gal detected represented a secreted product of the cells originally present in the porcine skin or cellular debris retained following decellularisation.<sup>18</sup> Whether the presence of residual alpha-gal would lead to an adverse response to the acellular porcine dermis, if used clinically, is a matter of conjecture. Implanting cellular

xenografts that express the alpha-gal epitope results in hyperacute rejection.<sup>19</sup> However, it is not clear what effect residual alpha-gal, present in acellular scaffolds, has on the host response. There is evidence to suggest it does not have an adverse effect on the tissue remodelling of decellularised xenogeneic tissue.<sup>18</sup> Recent research has also indicated that wound healing may be accelerated by the interaction of non-cellular alpha-gal with anti-alpha-gal antibodies.<sup>20</sup> Wounds treated with alpha-gal nanoparticles demonstrated a 40%–60% decrease in healing time compared to control wounds treated with saline.<sup>20</sup> By definition, decellularised human dermis should not contain the alpha-gal epitope. The presence of small areas of focal staining in decellularised human dermis, from one human donor, is likely to be caused by non-specific binding by biotinylated GSL-1 isolectin B<sub>4</sub>. Biotinylated GSL-1 isolectin B<sub>4</sub> labels alpha-galactosyl residues but can also bind to non-peptidergic unmyelinated primary afferent neurons and mast cells in human skin.<sup>21</sup>

In addition to removing major cellular antigens, decellularisation processes also aim to preserve the integrity of the ECM and bound growth factors. Collagen is the most abundant protein in the dermal ECM and comprises approximately 70%–80% of its dry weight.<sup>22</sup> Histological analysis suggested there was no change to the distribution of collagen fibres following decellularisation of the porcine dermis. In decellularised human dermis, the distribution of collagen fibres appeared less dense. This may have been due to variation between species and also the difference in the age of the tissue source. Decellularised porcine dermis was produced from skin from 6-month-old donors, whereas the mean age of the human skin donors was 63 years. The rate of collagen synthesis and the thickness of collagen fibre bundles in human skin have been reported to decrease with age.<sup>22,23</sup>

Since hydroxyproline is largely restricted to collagen, determination of hydroxyproline content can be used as an indicator of the collagen content in tissue. The concentration of hydroxyproline was significantly higher in decellularised porcine dermis than native cellular porcine skin. This was most likely caused by a relative increase in the ratio of hydroxyproline to total dry weight, following removal of cellular components. While histological analysis identified differences in the distribution of collagen fibres between decellularised porcine dermis and decellularised human dermis, there was no significant difference in the concentration of hydroxyproline between the two acellular scaffolds.

Elastin is also a major structural protein in the ECM. The decellularisation protocol developed during this study did not lead to visible changes to the distribution of elastin fibres in porcine dermis. Qualitative assessment of elastin fibres suggested higher intensity of staining in decellularised human dermis compared to decellularised porcine dermis. Further analysis would be required to determine whether decellularised human dermis contains higher

levels of elastin by quantifying using an elastin assay.<sup>24</sup> Potential differences in elastin concentration may also be attributed to the age of the tissue source. Elastin in human skin has been reported to undergo a number of age-related changes, including increased synthesis of abnormal elastin, particularly in photo-exposed areas.<sup>22</sup>

Immunohistochemical analysis of the basement membrane showed that collagen IV staining was no longer visible in acellular porcine dermis following decellularisation but was present in decellularised human dermis. Positive staining of laminin was visible in cellular porcine skin and both acellular scaffolds. Disruption of collagen IV immunostaining in decellularised porcine dermis was likely to be caused by PAA disinfection. PAA has been shown to diminish immunohistochemical staining of collagen IV, following decellularisation of human femoral arteries.<sup>25</sup> The decellularised human dermis characterised in this study was produced by National Health Service Blood and Transplant (NHSBT) using a method of decellularisation that had been adapted to omit the use of PAA.<sup>10</sup> This, therefore, could explain why collagen IV remained visible in the decellularised human dermis. It is important to note that, while collagen IV staining was present in decellularised human dermis, it was only visible at the dermo-epidermal junction in one of three human donors. Given that the tissue was analysed by staining cross-sectional tissue sections, it was not possible to determine whether the same pattern of staining would be seen across the entire surface of samples. These observations do, however, suggest that there may be other steps in the decellularisation process that cause collagen IV disruption at the dermo-epidermal junction, such as during the removal of the epidermis.

Mechanical properties of tissues are directly related to the structural components of the ECM and how they are arranged.<sup>26</sup> There were no significant differences between cellular porcine skin and decellularised porcine dermis for any of the biomechanical parameters studied. This suggested the mechanical properties of the porcine dermis were unaffected by the decellularisation process developed during this study. Analysis of acellular scaffolds showed that the mean thickness of decellularised porcine dermis was significantly higher than decellularised human dermis. This was likely to be due to differences in the thickness setting of the dermatome used in the porcine decellularisation protocol compared to the human protocol. There were no significant differences between the decellularised porcine, cellular porcine and decellularised human dermis in the biomechanical parameters of UTS, collagen phase, elastin phase and maximum load. While there were no significant differences in biomechanical parameters across the three groups, there was considerable variation between the donors in the decellularised porcine dermis group. This was potentially due to tissue being inadvertently taken from a different site. There have been reports of variation in the mechanical properties of animal and human skin depending on the location of the tissue.<sup>27</sup>

There have been other studies that have reported the development of a decellularised porcine dermis. Chen et al.<sup>28</sup> used a method of decellularisation that included trypsin, dispase II and SDS. However, this study did not appropriately analyse whether the cells had been adequately removed. Assessment of cell removal was based on qualitative observation of H&E-stained tissue sections<sup>28</sup> with no DNA content analysis. Prasertsung et al.<sup>29</sup> decellularised porcine dermis using dispase II, in combination with a periodic pressurised technique. The periodic pressurised technique reduced the enzymatic incubation time required. While this technique decreased the incubation time of enzymatic treatments, the decellularisation process still involved treatment with 85% glycerol for 14 days. This made the overall process lengthy and much longer than the 4.5 days taken to decellularise porcine dermis in this study. There was also no assessment of the effect of the periodic pressurised technique and dispase II on the mechanical properties of the acellular dermis.<sup>29</sup>

## Conclusion

This study reports the development of a decellularised porcine dermis, using a method of decellularisation that uses low-concentration 0.1% (w/v) SDS and proteinase inhibitors. It was hypothesised that a decellularised porcine dermis produced using this method would not cause any changes to the biological, biochemical or biomechanical properties of the native tissue. The results from this study support this hypothesis; however, there was considerable variation in the biomechanical properties, particularly in the decellularised porcine dermis group and diminished collagen IV staining.

## Acknowledgements

We are grateful for the kindness of donors and donor families for the donation of human tissue used during this study. The data for this study are freely available in the Leeds Data Repository <https://doi.org/10.5518/177>.

## Declaration of conflicting interests

E.I. is a consultant to and holds equity in Tissue Regenix Group PLC.

## Funding

J.A.H. was supported through the Royal College of Physicians Wolfson award funded by the Wolfson Foundation. This work was also partly supported through the Leeds Centre of Excellence in Medical Engineering funded by the Wellcome Trust and EPSRC, WT088908/z/09/z. E.I. is supported by NIHR Leeds Musculoskeletal Biomedical Research Unit.

## References

1. Palfreyman S. Assessing the impact of venous ulceration on quality of life. *Nurs Times* 2008; 104(41): 34–37.
2. SIGN. *Management of chronic venous leg ulcers SIGN guidelines*, 2010, <http://www.sign.ac.uk/assets/sign120.pdf>

3. Turner NJ and Badylak SF. The use of biologic scaffolds in the treatment of chronic nonhealing wounds. *Adv Wound Care* 2015; 4(8): 490–500.
4. Hogg P, Rooney P, Ingham E, et al. Development of a decellularised dermis. *Cell Tissue Bank* 2013; 14(3): 465–474.
5. Bolland F, Korossis S, Wilshaw SP, et al. Development and characterisation of a full-thickness acellular porcine bladder matrix for tissue engineering. *Biomaterials* 2007; 28(6): 1061–1070.
6. Stapleton TW, Ingram J, Katta J, et al. Development and characterization of an acellular porcine medial meniscus for use in tissue engineering. *Tissue Eng Part A* 2008; 14(4): 505–518.
7. Kheir E, Stapleton T, Shaw D, et al. Development and characterization of an acellular porcine cartilage bone matrix for use in tissue engineering. *J Biomed Mater Res A* 2011; 99(2): 283–294.
8. Greaves NS, Benatar B, Baguneid M, et al. Single-stage application of a novel decellularized dermis for treatment-resistant lower limb ulcers: positive outcomes assessed by SIAscopy, laser perfusion, and 3D imaging, with sequential timed histological analysis. *Wound Repair Regen* 2013; 21(6): 813–822.
9. Greaves NS, Lqbal SA, Morris J, et al. Acute cutaneous wounds treated with human decellularised dermis show enhanced angiogenesis during healing. *PLoS ONE* 2015; 10(1): e0113209.
10. Hogg P, Rooney P, Leow-Dyke S, et al. Development of a terminally sterilised decellularised dermis. *Cell Tissue Bank* 2015; 16(3): 351–359.
11. Fermor HL, Russell SL, Williams S, et al. Development and characterisation of a decellularised bovine osteochondral biomaterial for cartilage repair. *J Mater Sci Mater Med* 2015; 26(5): 186.
12. Crapo PM, Gilbert TW and Badylak SF. An overview of tissue and whole organ decellularization processes. *Biomaterials* 2011; 32(12): 3233–3243.
13. Shevchenko RV, James SL and James SE. A review of tissue-engineered skin bioconstructs available for skin reconstruction. *J R Soc Interface* 2010; 7(43): 229–258.
14. Wilcox HE, Korossis SA, Booth C, et al. Biocompatibility and recellularization potential of an acellular porcine heart valve matrix. *J Heart Valve Dis* 2005; 14(2): 228–236; discussion 236–237.
15. Korossis SA, Wilcox HE, Watterson KG, et al. In-vitro assessment of the functional performance of the decellularized intact porcine aortic root. *J Heart Valve Dis* 2005; 14(3): 408–421; discussion 422.
16. Baiguera S, Jungebluth P, Burns A, et al. Tissue engineered human tracheas for in vivo implantation. *Biomaterials* 2010; 31(34): 8931–8938.
17. Keane TJ, Swinehart IT and Badylak SF. Methods of tissue decellularization used for preparation of biologic scaffolds and in vivo relevance. *Methods* 2015; 84: 25–34.
18. Badylak SF and Gilbert TW. Immune response to biologic scaffold materials. *Semin Immunol* 2008; 20(2): 109–116.
19. Bucher P, Morel P and Buhler LH. Xenotransplantation: an update on recent progress and future perspectives. *Transpl Int* 2005; 18(8): 894–901.
20. Galili U. Acceleration of wound healing by alpha-gal nanoparticles interacting with the natural anti-Gal antibody. *J Immunol Res* 2015; 2015: 589648.
21. Lonne-Rahm S, El-Nour H and Aldskogius H. Bandeiraea simplicifolia isolectin B4 binds mast cells in human skin and this latter binding is up-regulated in patients with atopic dermatitis and stinging. *J Clin Exp Dermatol Res* 2012; 3: 156.
22. Waller JM and Maibach HI. Age and skin structure and function, a quantitative approach (II): protein, glycosaminoglycan, water, and lipid content and structure. *Skin Res Technol* 2006; 12(3): 145–154.
23. Lovell CR, Smolenski KA, Duance VC, et al. Type I and III collagen content and fibre distribution in normal human skin during ageing. *Br J Dermatol* 1987; 117(4): 419–428.
24. Wilshaw SP, Kearney JN, Fisher J, et al. Production of an acellular amniotic membrane matrix for use in tissue engineering. *Tissue Eng* 2006; 12(8): 2117–2129.
25. Wilshaw SP, Rooney P, Berry H, et al. Development and characterization of acellular allogeneic arterial matrices. *Tissue Eng Part A* 2012; 18(5–6): 471–483.
26. Silver F and Christiansen D. *Biomaterials science and biocompatibility*. New York: Springer Science & Business Media, 1999.
27. Gallagher A, Anniadh N, Bruyere K, et al. Dynamic tensile properties of human skin. In: *Proceedings of the IRCOBI conference 2012*, Dublin, 12–14 September 2012.
28. Chen RN, Ho HO, Tsai YT, et al. Process development of an acellular dermal matrix (ADM) for biomedical applications. *Biomaterials* 2004; 25(13): 2679–2686.
29. Prasertsung I, Kanokpanont S, Bunaprasert T, et al. Development of acellular dermis from porcine skin using periodic pressurized technique. *J Biomed Mater Res B Appl Biomater* 2008; 85(1): 210–219.